

# 1/8 Doping Anomalies and Oxygen Vacancies in Underdoped Superconducting Cuprates

Joshua L. Cohn

*Department of Physics, University of Miami, Coral Gables, FL 33124*

**Abstract.** Measurements of thermal conductivity ( $\kappa$ ) versus temperature and doping for several cuprate superconductors are discussed. Suppressed values of the normal-state  $\kappa$  and the slope change in  $\kappa$  at  $T_c$ , observed near 1/8 doping in both  $\text{YBa}_2\text{Cu}_3\text{O}_{6+x}$  and Hg cuprates, are attributed to local lattice distortions and the suppression of the superconducting condensate, respectively. Both phenomena are proposed to arise from small domains of localized planar holes, presumably a manifestation of phase separation. It is suggested that the phase behavior of  $\kappa$  reflects stripe dynamics and the 1/8 doping anomalies stripe pinning by oxygen-vacancy clusters.

## INTRODUCTION

There is mounting experimental evidence that novel charge- and spin-ordered phases are generic to underdoped cuprates [1]. The doped holes in Nd-doped  $\text{La}_{1-x}\text{Sr}_x\text{CuO}_4$  segregate into periodic stripes that separate antiferromagnetically ordered, hole-poor domains. Lattice distortions pin these stripes, and this pinning is most effective for planar hole concentrations near  $p=1/8$  where the stripe modulation wavelength is commensurate with the lattice. In the absence of pinning, stripe modulations are presumed to be fluctuating and/or disordered, and this is the emerging picture for  $\text{La}_{1-x}\text{Sr}_x\text{CuO}_4$  (La-214) and  $\text{YBa}_2\text{Cu}_3\text{O}_{6+x}$  (Y-123) [2]. We have recently demonstrated, through measurements of thermal conductivity ( $\kappa$ ) [3], that both Y-123 and  $\text{HgBa}_2\text{Ca}_{m-1}\text{Cu}_m\text{O}_{2m+2+\delta}$  [Hg-12( $m-1$ ) $m$ ,  $m=1, 2, 3$ ] exhibit doping anomalies near  $p=1/8$  that can be attributed to the presence of localized charge and associated lattice distortions. Here we discuss the oxygen doping behavior of the anomalies in Hg cuprates and present new results on vacancy-free Ca-doped  $\text{YBa}_2\text{Cu}_4\text{O}_8$  (Y-124) that suggest elastic properties may reflect stripe dynamics and stripe fragments may pin near oxygen-vacancy clusters.

The  $p=1/8$  features (Fig. 1) are evident in the doping behavior of the normal-state thermal resistivity,  $W = 1/\kappa$ , and the normalized change in temperature derivative of  $\kappa$  that occurs at  $T_c$ ,  $\Gamma \equiv -d(\kappa^s/\kappa^n)/dt|_{t=1}$  [ $t = T/T_c$  and  $\kappa^s(\kappa^n)$  is the thermal conductivity in the superconducting (normal) state]. For Y-123, there is

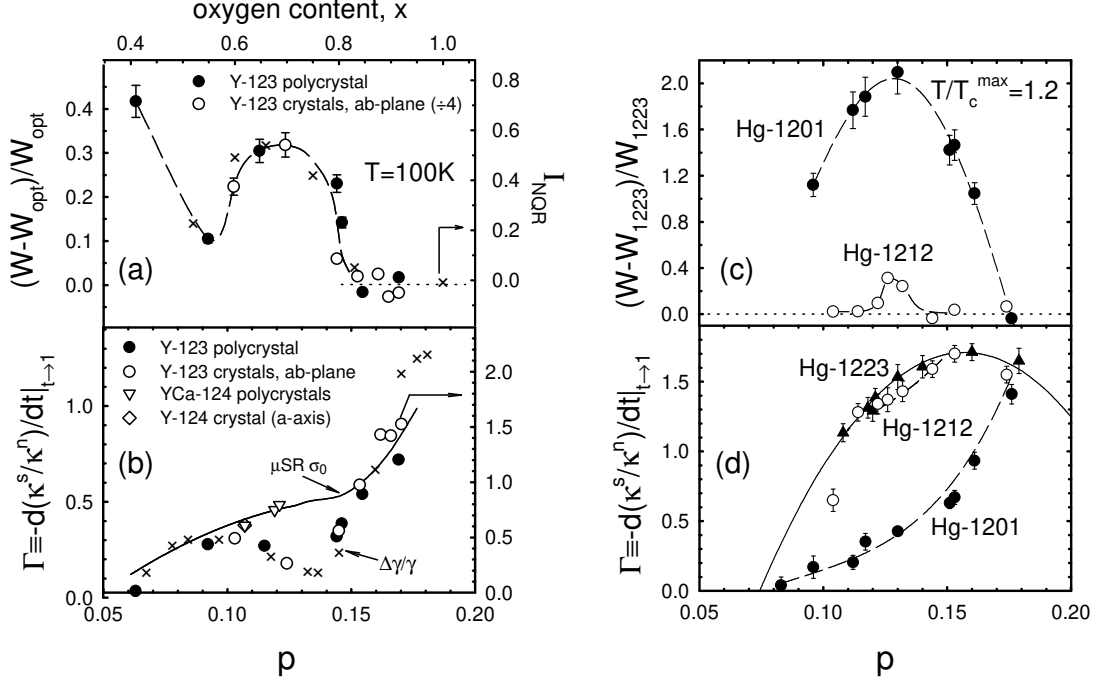


**FIGURE 1.** (a) Thermal resistivity at  $T=100\text{K}$  relative to that at  $p_{opt} = 0.16$  for Y-123 polycrystals and the ab-plane of single crystals [4] [ $W_{opt} = 0.21 \text{ mK/W}$  ( $0.08\text{mK/W}$ ) for the polycrystal (crystals)]. The hole concentration per planar Cu atom,  $p$ , was determined from thermopower measurements and the empirical relations with bond valence sums 59 established by Tallon *et al.* [5]. Also plotted ( $\times$ 's) is the relative intensity of anomalous  $^{63}\text{Cu}$  NQR signals [6]. The dashed curve is a guide to the eye. (b) The normalized slope change in  $\kappa(T)$  at  $T_c$  vs doping for each of the Y-123 specimens in (a), for the a-axis of single-crystal Y-124 [7], and for polycrystal  $\text{Y}_{1-x}\text{Ca}_x\text{-124}$  [8]. The  $\text{Y}_{1-x}\text{Ca}_x\text{-124}$  data are multiplied by 2.3 so that they coincide with the Y-124 crystal data at  $x=0$ . Solid (open) symbols are referred to the left (right) ordinate. Also shown ( $\times$ 's) are the normalized electronic specific heat jump [9],  $\Delta\gamma/\gamma$ , and (solid curve) the  $\mu\text{SR}$  depolarization rate [10] (in  $\mu\text{s}^{-1}$ ), divided by 1.4 and 2.7, respectively, and referred to the right ordinate. (c) Thermal resistivity for Hg-1201 and Hg-1212 polycrystals relative to that of Hg-1223 [3]. Dashed curves are guides. (d) The normalized slope change in  $\kappa(T)$  at  $T_c$  vs doping for Hg cuprates. The solid line is  $1.71 - 250(p - 0.157)^2$ . Dashed curves are guides.

a compelling correlation of  $W(p)$  and  $\Gamma(p)$  with the doping behavior of anomalous  $^{63}\text{Cu}$  NQR spectral weight [6], attributed to localized holes, and the electronic specific heat jump [9],  $\Delta\gamma/\gamma$ , respectively [crosses in Fig.'s 1 (a) and (b)]. Thus  $W$  probes lattice distortions associated with localized holes, and  $\Gamma$  the change in low-energy spectral weight induced by superconductivity.

Since both  $\Gamma$  and  $\Delta\gamma/\gamma$  provide bulk measures of the superfluid volume, it is significant that the muon spin rotation ( $\mu\text{SR}$ ) depolarization rate [ $\sigma_0$  in Fig. 1

(b)], proportional to the superfluid density, exhibits no anomalous behavior near  $1/8$  doping. The  $\mu$ SR signal originates in regions of the specimen where there is a flux lattice. The apparent discrepancy between  $\sigma_0$  and  $\Gamma$  or  $\Delta\gamma/\gamma$  is resolved if the material is inhomogeneous, composed of non-superconducting clusters embedded in a superconducting network. The suppression of  $\Gamma$  and  $\Delta\gamma/\gamma$  below the scaled  $\sigma_0$  curve in Fig. 1 (a) are then measures of the non-superconducting volume fraction. Taken together, the  $W$  and  $\Gamma$  data imply that the non-superconducting regions are comprised of localized holes and associated lattice distortions, i.e. polarons. It is plausible that these hole-localized regions are stripe domains akin to those inferred from neutron scattering [1]. That they produce lattice thermal resistance implies they are static on the timescale of the average phonon lifetime, estimated as a few ps in the ab-plane of Y-123 [3]. Given that  $T_c$  is not substantially suppressed near  $p=1/8$  implies that these regions do not percolate, and thus the picture is one of small clusters of localized holes and their associated lattice distortions, perhaps no larger than the stripe unit cell ( $2a \times 8a$  where  $a$  is the lattice constant [1]), separated by a distance comparable to the phonon mean free path (about  $100\text{\AA} \sim 25a$  at 100K).

For the Hg materials the  $p=1/8$  enhancement of  $W$  and suppression of  $\Gamma$  is most prominent in single-layer Hg-1201, less so in double-layer Hg-1212, and absent or negligible in three-layer Hg-1223. This trend follows that of the oxygen vacancy concentration: a single  $\text{HgO}_\delta$  layer per unit cell contributes charge to  $m$  planes in  $\text{Hg-12}(m-1)m$  so that the oxygen vacancy concentration,  $1 - \delta$ , increases with decreasing  $m$  [11]. The absence of suppression in  $\Gamma$  near  $1/8$  doping for Hg-1223 [Fig. 1 (d)] suggests that this material has sufficiently few localized-hole domains that their effects in  $W$  and  $\Gamma$  are unobservable. Thus we employ the Hg-1223  $W(p)$  data as a reference and plot the differences for the other two compounds in Fig. 1 (c). Comparing Fig.'s 1 (c) and (d) we see that for both Hg-1201 and Hg-1212  $W$  is enhanced and  $\Gamma$  is suppressed relative to values for Hg-1223 in common ranges of  $p$ , with maximal differences near  $p=1/8$ .

## STRIPES ALTER THE PHONON DISPERSION?

That  $1/8$  doping anomalies are observed in both Y-123 and Hg cuprates suggests they are a generic feature of underdoped  $\text{CuO}_2$  planes. In this context the doping behavior of  $\kappa$  for Hg-1223 [Fig. 2 (a)] is of interest since it presumably approximates the phase behavior in the absence of localized holes. We expect the electronic contribution,  $\kappa_e$ , to increase smoothly with increasing  $p$ . The upturn in  $\kappa$  above optimal doping ( $p=0.16$ ) is presumably attributable to this rising  $\kappa_e$ . The most reliable estimate of  $\kappa_e$  in the cuprates comes from thermal Hall conductivity measurements [12] on Y-123 which imply  $\kappa_e/\kappa \simeq 0.1$  for in-plane heat conduction near optimal doping. The data in Fig. 1 (a), (b) suggest that this ratio is roughly the same in polycrystals, thus motivating the dotted and dashed curves in Fig. 2 (a) as an educated guess for the electronic and lattice terms, respectively, in Hg-1223.

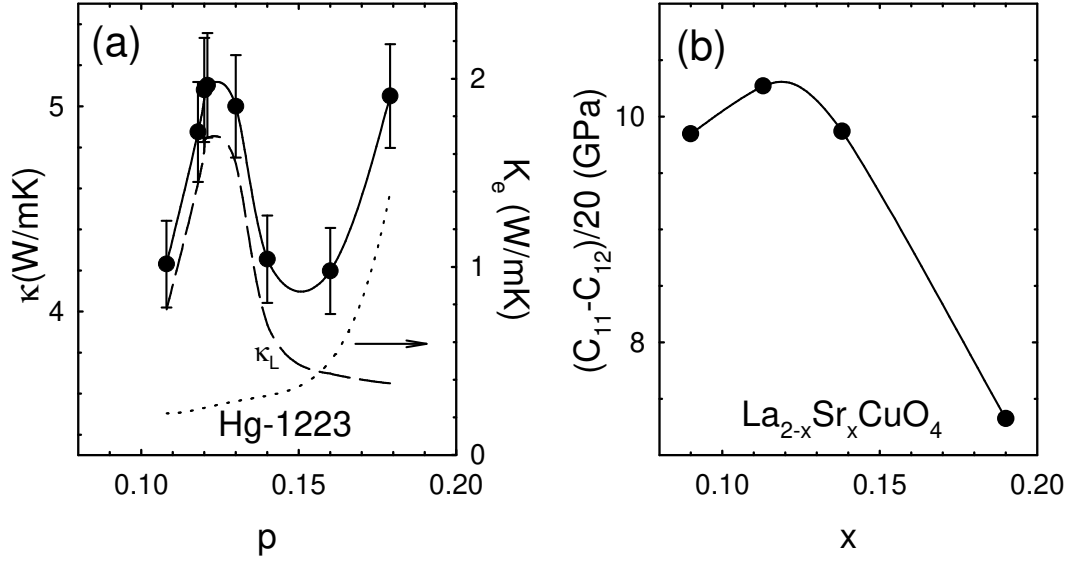


**FIGURE 2.** (a) Thermal conductivity of Hg-1223 polycrystal versus doping. The dotted and dashed curves are proposed electronic (right ordinate) and lattice thermal conductivities, respectively. The solid line is a guide to the eye. (b) sound velocity data for single-crystal La-214 from Ref. [13].

The lattice conductivity,  $\kappa_L = \kappa - \kappa_e$ , predominates in the underdoped regime and is peaked near  $p=1/8$ .

There is experimental support for the proposal that this peak in  $\kappa$  is associated with doping-dependent changes in the phonon dispersion which are generic to underdoped cuprates. Figure 2 (b) shows the behavior of the normal-state, transverse shear elastic constant (proportional to the square of the sound velocity) for single-crystal La-214 [13], the only material for which doping-dependent measurements for all the main symmetry directions have been reported to our knowledge. A substantial hardening of the lattice in the underdoped regime, with a maximum near  $p = x \simeq 1/8$ , was observed for all symmetries, indicating that the changes with doping are systemic.

It is possible that the phase behavior of the elastic constants for La-214 and  $\kappa_L$  for Hg-1223 reflect a renormalization of the lattice dispersion due to changes in stripe dynamics with doping. At  $p=1/8$  the stripes are maximally commensurate with the lattice, and their fluctuations should be minimal. Enhanced fluctuations are to be expected at higher doping, due to the destabilizing role of repulsive interactions in stripes that neutron scattering results (Yamada *et al.* [2]) suggest, are charge compressed. For  $p < 1/8$ , the cluster spin-glass state observed by  $\mu$ SR studies [14] is characterized by increasing magnetic disorder with decreasing  $p$  in the range

$0.08 < p < 0.12$ , possibly associated with increasing disorder [15] in the stripe period. It is plausible that disorder in the stripe system at both higher and lower doping about  $p=1/8$  induces a softening of the lattice that is reflected in Fig. 2. Theoretical investigations of elastic coupling to the stripe system would certainly be of interest.

## OXYGEN VACANCIES AND 1/8 ANOMALIES

Returning now to the enhancement of  $W$  and suppression of  $\Gamma$  near  $p=1/8$ , our measurements suggest these phenomena reflect stripe pinning (or reduced stripe fluctuations) associated with oxygen vacancy clusters. Raman studies of defect modes in the Hg materials [16] provide a measure of the density of vacancy clusters. The  $590\text{ cm}^{-1}$  Raman mode in Hg cuprates is attributed to c-axis vibrations of apical oxygen in the presence of oxygen vacancies on each of the four nearest-neighbor sites in the  $\text{HgO}_\delta$  layers. The amount by which the thermal resistivity and  $\Gamma$  values of Hg-1201 and Hg-1212 differ from those of Hg-1223 at  $p=1/8$  both correlate well with the integrated oscillator strength of this vibrational mode normalized by that of the  $570\text{ cm}^{-1}$  mode (Fig. 3), the latter attributed to apical vibrations in the presence of fewer than four vacancies, and common in the spectra [16] of all three Hg materials. We infer that oxygen-vacancy clusters, of size four or more in the Hg cuprates, can pin a stripe fragment.

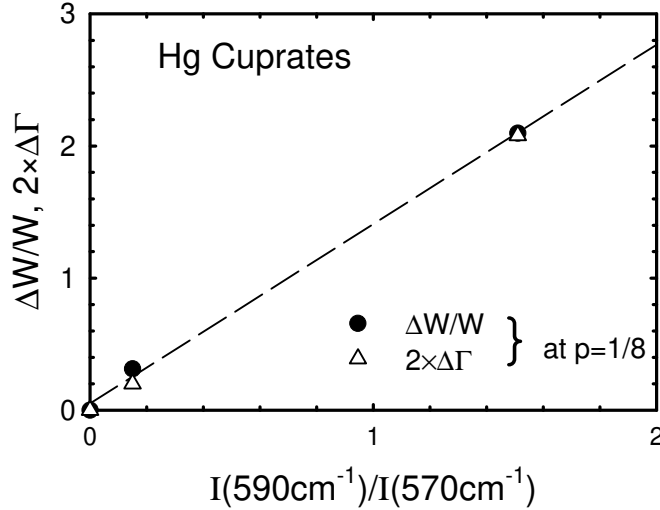


**FIGURE 3.** (a) The enhancement in thermal resistivity and suppression in  $\Gamma$  for the Hg compounds at  $p=1/8$ , relative to values for Hg-1223, plotted versus the oscillator strength ratio of Raman-scattering defect modes (Ref. [16]).

Supporting the role of oxygen vacancies in the observed  $1/8$  features for Y-123 are our recent measurements on oxygen-stoichiometric  $Y_{1-x}Ca_x$ -124 [8]. The  $\Gamma$  values for  $x=0, 0.10, 0.15$  are plotted in Fig. 1 (b). There is no evidence for suppression of  $\Gamma$  near  $1/8$  doping, and the data follow the scaled  $\mu$ SR curve quite well. Within the context of the interpretation we have outlined, we conclude that Ca substitution for Y (at the level of  $\leq 15\%$ ) is not as effective in stripe pinning as are oxygen vacancy clusters. It remains to be determined by what mechanism these clusters induce pinning.

## ACKNOWLEDGEMENTS

This work was supported by NSF Grant No. DMR-9631236.

## REFERENCES

1. J. M. Tranquada *et al.*, Nature **375**, 561 (1995); Phys. Rev. Lett.**78**, 338 (1997); T. Suzuki *et al.*, Phys. Rev. B **57**, R3229 (1998).
2. J. M. Tranquada, J. Phys. Chem. Solids **59**, 2150 (1998); H. Mook *et al.*, Nature **395**, 580 (1998); P. Dai *et al.*, Phys. Rev. Lett.**80**, 1738 (1998); K. Yamada *et al.*, Phys. Rev. B **57**, 6165 (1998).
3. J. L. Cohn *et al.*, Phys. Rev. B**59**, 3823 (1999).
4. C. P. Popoviciu and J. L. Cohn, Phys. Rev. B **55**, 3155 (1997); J. L. Cohn, *ibid.* **53**, R2963 (1996).
5. J. L. Tallon *et al.*, Phys. Rev. B **51**, 12911 (1995).
6. P. C. Hammel and D. J. Scalapino, Phil. Mag. **74**, 523 (1996); H. Yasuoka *et al.*, Phase Trans. **15**, 183 (1989).
7. J. L. Cohn and J. Karpinski, Phys. Rev. B**58**, 14617 (1998).
8. J. L. Cohn *et al.*, unpublished.
9. J. W. Loram *et al.*, Phys. Rev. Lett.**73**, 1721 (1993).
10. Y. J. Uemura *et al.*, Phys. Rev. Lett.**66**, 2665 (1991); J. L. Tallon *et al.*, *ibid.* **74**, 1008 (1995).
11. O. Chmaissem *et al.*, Physica C **217**, 265 (1993); E. V. Antipov *et al.*, *ibid.* **218**, 348 (1993); Q. Huang *et al.*, Phys. Rev. B **52**, 462 (1995).
12. K. Krishana *et al.*, Phys. Rev. Lett.**75**, 3529 (1995).
13. S. Sakita *et al.*, Physica B **219-220**, 216 (1996); M. Nohara *et al.*, Phys. Rev. B**52**, 570 (1995).
14. Ch. Niedermayer *et al.*, Phys. Rev. Lett. **80**, 3843 (1998).
15. S. A. Kivelson and V. J. Emery, cond-mat/9809082.
16. X. Zhou *et al.*, Phys. Rev. B **54**, 6137 (1996).